Thermo-economic optimization of an adiabatic compressed air energy storage system. Influence of turbomachinery and materials

David Pérez-Gallego[a,b], Alejandro Medina[a,b], Julián González-Ayala[a,b], Antonio Calvo Hernández[a,b]

[a] *Department of Applied Physics, University of Salamanca, Salamanca, 37008, Castilla y León, España, dpgallego@usal.es*

[b] *Instituto Universitario de Física Fundamental y Matemáticas (IUFFyM), University of Salamanca, Salamanca, 37008, Castilla y León, España*

Abstract:

This paper is focused on the modeling of an adiabatic compressed air energy storage plant (ACAES). This type of plant utilizes surplus energy from the grid (high photovoltaic or wind production) or periods of low electricity prices to compress air using a compression train. During compression, the air increases its temperature. The thermal energy is stored in a packed-bed system, which consists of a rock reservoir through which air flows and gets cooler as the rock heats up. The compressed air is stored in an isochoric, sealed cavern. When demand or electricity price rises, the compressed air cavern is discharged. The air flows back through the packed-bed systems, where its temperature increases. The air then generates electricity in the plant's turbines. This work has a dual objective. First, to fully model and simulate the operation of this type of plant, solving the dynamic equations in an integrated manner for all components. This model allows us to analyze the thermodynamic behavior of the ACAES plant and its efficiency. The second objective of this work is to estimate the initial capital expenditures (CAPEX) and the levelized cost of storage (LCoS) to amortize the plant over a 30-year useful life. To reach this goal, a multi-objective optimization (using the NSGA-II algorithm) of the main parameters is performed to obtain the Pareto front for LCoS/CAPEX. LCoS prices of around €90/MWh are obtained for an electricity charge price of €50/MWh, which ensures promising profitability since the market graph establishes higher prices in certain time ranges.

Keywords:

Centrifugal compressors; Compressed air; Energy storage; Radial packed-beds; Thermal energy storage.

1. Introduction

Photovoltaic (PV) and wind energy production are well established within the electrical power system. Concentrated solar thermal energy is somewhat less consolidated; however, it has the advantage of incorporating an intrinsic energy storage method based, for instance, on molten salts. One of the main limitations of PV or wind systems is energy storage during periods of high production, particularly during hours of peak solar irradiance. Numerous storage methods have been proposed, with lithium-ion batteries standing out due to their high efficiency. However, lithium is a relatively scarce material, and therefore alternative solutions must be considered. In this work, a compressed-air and thermal (adiabatic) energy storage system (ACAES) is investigated. In these plants, referred to as ACAES, ambient air is compressed through a compression train and stored at high pressure in an underground cavern. This stage corresponds to the charging phase. When required by demand, the compressed air is released from the cavern and expanded through turbines to generate electricity again. During the charge/discharge process, the air must be cooled prior to storage in the cavern and subsequently heated during discharge before entering the turbines. This process can be carried out by means of heat exchangers that cool the air prior to cavern storage, and by natural-gas combustion chambers that heat the air before turbine expansion. Plants operating in this manner are known as Diabatic-CAES systems. Currently, only two large-scale commercial CAES (Compressed Air Energy Storage) plants exist worldwide: one in Huntorf, Germany, and the other in McIntosh, Alabama, USA. The Huntorf plant has a charging power capacity of 60 MWh and a discharging power capacity of 290 MWh. The respective charging and discharging durations are approximately 12 hours and 3 hours. The facility was constructed on a salt dome, which is used as the underground air-storage cavern. This installation will serve as the reference plant for the analysis conducted in this study.

Alternatively, in order to avoid the use of fossil fuels, thermal energy storage systems of the packed-bed type can be employed. These systems cool the air during the charging phase while storing the extracted thermal energy, and subsequently reheat the air during discharge before turbine expansion; these plants are referred to as Adiabatic-CAES systems. This type of storage technology has been only minimally explored: currently, there are only two commercial compressed-air plants operating with combustion chambers and none at a commercial scale operating in adiabatic mode, i.e., with an integrated thermal storage system [1]. Likewise, there are very few studies addressing the dynamic behavior of such plants [2], and analyses of their economic feasibility are almost non-existent [3]. For this reason, the present work focuses on two main objectives. The first is to model the dynamic operation and integration of all plant components. Based on this thermodynamic analysis, the second objective is to carry on a multi-objective optimization on the initial decision parameters related to plant sizing. This multi-objective optimization provides a thermo-economic trade-off between the initial capital investment (CAPEX) and the minimum selling price required to recover the investment, expressed as the Levelized Cost of Storage (LCoS). The aim is to minimize both objective functions and compare the resulting values with the current market landscape. In economic studies of this type, it is common practice to assume a constant electricity purchase price during the charging phase, typically set at 50 €/MWh. Such an analysis has previously been carried out [4].

2. Methodology

In this section, the methodology adopted to model an ACAES-type compressed air energy storage plant is described. Once the computational model has been developed and its performance validated, the economic analysis can be carried out. The fundamental objective is to simultaneously reduce both the electricity selling price, expressed as the Levelized Cost of Storage (LCoS), and the initial capital investment (CAPEX).

2.1. Adiabatic compressed air energy storage

The ACAES plant configuration considered in this study is shown in Fig. 1. During periods when electricity prices are low, the plant compressors begin compressing ambient air, increasing both its pressure and temperature. The thermal energy generated during compression is stored in packed-bed thermal storage systems for subsequent recovery, while the high-pressure air is stored in an underground cavern, typically of saline origin (although other options such as abandoned mines or depleted natural gas reservoirs may also be used). During periods of the day when the electricity price—or demand—increases, the ACAES plant operates in discharge mode, recovering the energy stored during the charging phase. In this stage, the high-pressure air leaves the cavern, its temperature rises as it flows through the packed-bed thermal storage units, and it then expands through turbines, generating electrical power in the process. In a previous study [4], several ACAES plant configurations were analyzed, including systems with one or two packed-bed units and configurations incorporating a Rankine cycle between turbines to recover residual heat. The plant configuration analyzed in the present work is shown in Fig. 1. This configuration demonstrated a high overall efficiency, or round-trip efficiency (RTE), while avoiding additional components that would increase the plant cost, such as an Organic Rankine Cycle (ORC).

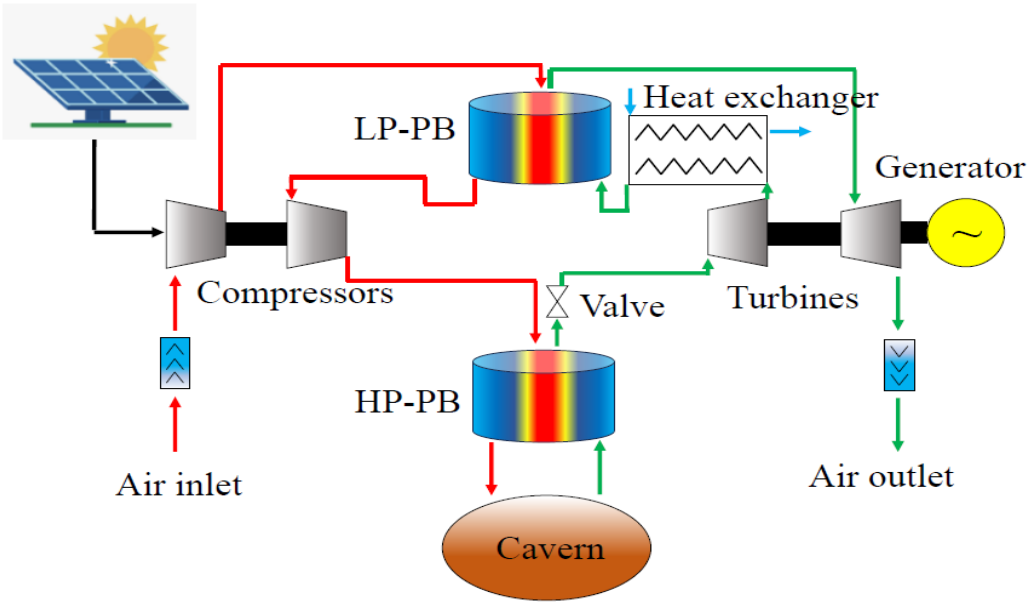

Figure 1. *Schematic diagram of a double packed-bed ACAES plant.*

2.2. Packed-bed

A packed-bed system for thermal energy storage consists of a bed of high-heat-capacity solid rock material through which a heat-carrying fluid—in this case, air—is circulated. During the charging phase, the hot fluid transfers its thermal energy to the solid bed, raising its temperature and storing energy sensibly or latently if phase-change storage materials are employed. During the discharging phase, cold air flows through the hot bed, recovering the stored thermal energy and conveying it to the turbines for electricity generation. This type of system is notable for its simplicity, high energy density, and ability to operate in repeated cycles with relatively low thermal losses. Packed-bed systems are modeled using the Schumann heat transfer equations between air and the solid medium, the mass conservation equation, and the Ergun equation for pressure drops (momentum conservation), Eqs. (1)–(4). These equations are solved using finite differences with the implicit Euler method (see [4] for details).

$$\varepsilon\rho_f c_{p,f}\left(\frac{\partial T_f}{\partial t}+u\frac{\partial T_f}{\partial z}\right)=\frac{\partial}{\partial z}\left(K_f\frac{\partial T_f}{\partial z}\right)+ha_s\left(T_s-T_f\right)+Ua_b\left(T_\infty-T_f\right), \quad (1)$$

$$(1-\varepsilon)\rho_s c_{p,s}\left(\frac{\partial T_s}{\partial t}\right)=\frac{\partial}{\partial z}\left(K_s\frac{\partial T_s}{\partial z}\right)+ha_s\left(T_f-T_s\right), \quad (2)$$

$$\left(\frac{\partial \rho_f}{\partial t}\right)+\nabla\cdot\left(u\rho_f\right)=0, \quad (3)$$

$$\left(-\frac{\Delta P}{L}\right)=150\left(\frac{(1-\epsilon)^2}{\epsilon^3}\right)\left(\frac{\mu_f}{d_p^2}\right)u+1.75\left(\frac{1-\epsilon}{\epsilon^3}\right)\left(\frac{\rho_f}{d_p}\right)u^2. \quad (4)$$

In the above equations, the subscript “s” refers to the solid storage material, and “f” refers to the heat exchange fluid (air). Here, ε is the void fraction of the storage material, ρ is the density, c_p the heat capacity, K the thermal conductivity, h the convective heat transfer coefficient between the fluid and the solid, U an effective heat loss parameter, T_∞ the ambient temperature, u the fluid velocity, and ΔP the pressure drop. Further details can be found in [5]. Moreover, packed-bed thermal storage systems can be classified according to their geometry. There are two main types: axial and radial. The primary difference lies in the axis along which the air flows. In axial systems, the airflow is directed along the axial axis of the cylindrical packed-bed. In radial systems, the beds are still cylindrical but slightly flattened, and the airflow moves radially—from the center outward during charging, and in reverse during discharging. In this work, a radial packed-bed configuration is selected, as it provides lower pressure drops compared to axial beds, positively impacting the overall system efficiency [4].

2.3. High pressure air storage

The high-pressure air storage cavern is modeled using differential equations that describe the variation of mass and energy exchange with the surroundings. In practice, isochoric tanks or caverns are employed, so the thermodynamic variables of the system can be determined from the mass and energy conservation equations, except for the pressure, which is obtained using the ideal gas law. Heat transfer through the tank walls is characterized by an effective heat transfer coefficient, typically estimated by fitting to experimental data. Although this coefficient can be low in well-insulated systems, a perfectly adiabatic behavior is not achieved. Other configurations, such as isobaric tanks with approximately isothermal behavior under slow operational regimes, are not considered in this study. The differential equations for mass and energy transfer in the isochoric cavern, Eqs. (5)–(6), are also solved using the implicit Euler method.

$$m\,c_p\left(\frac{dT}{dt}\right)-\left(\frac{R\,T}{M}\right)(\dot{m}_c-\dot{m}_d)-\left(m\,\frac{R\,T}{M}\right)\left(\frac{dT}{dt}\right)=\dot{m}_c c_p(T_{in}-T)-h_{eff}(T-T_w), \quad (5)$$

$$\frac{dm}{dt}=\dot{m}_c-\dot{m}_d. \quad (6)$$

Here, R is the ideal gas constant, $\dot{m}_c$ is the mass flow rate during charging, $\dot{m}_d$ is the mass flow rate leaving the cavern during discharging, h_{eff} is the convective heat transfer coefficient between the air and the cavern, and T_w is the temperature of the cavern wall.

2.4. Turbomachinery

Axial and centrifugal compressors, such as those employed in this study, can be ideally described using the ideal gas law and the isentropic efficiency of the compressor. However, this idealization is of limited use because real compressors exhibit complex fluid-dynamic phenomena associated with rotor speed, and their efficiency is neither constant nor independent of operating conditions. Specifically, efficiency depends on the pressure ratio (r_p), the mass flow rate ($\dot{m}$), and the rotational speed (n). In high-pressure, constant-volume storage systems, compressors must operate efficiently over a wide range of elevated compression ratios to prevent backflow from the high-pressure reservoir, while handling variable air flows with approximately constant input power [2]. Axial compressors typically offer lower economic cost but operate over a narrower compression ratio range, whereas centrifugal compressors maintain acceptable efficiencies over a broader range. In CAES plants, a hybrid compression train is commonly used, consisting of a low-pressure axial compressor (LPC) followed by a high-pressure centrifugal compressor (HPC). The LPC raises the pressure from ambient conditions to an intermediate level at an approximately constant compression ratio, while the HPC further increases the pressure to the value required in the storage cavern, which varies as more air is injected. As the cavern pressure increases during the charging phase, the HPC must dynamically adjust its compression ratio. In this arrangement, the LPC typically operates at constant rotational speed, while the centrifugal HPC operates under off-design conditions. In this work, two compression train configurations are analyzed: the conventional hybrid arrangement (axial LPC + centrifugal HPC) and an alternative configuration using two centrifugal compressors. Although the latter entails higher capital cost, it provides an improvement in the overall round-trip efficiency (RTE) of the system. For centrifugal compressors, the optimal increase in compression ratio is achieved by adjusting the shaft speed and mass flow rate along the maximum efficiency operating line [6], which defines the points of maximum efficiency for each flow rate. In the simulations conducted here, this criterion is applied inversely: for each compression ratio, determined by the variable cavern pressure, the mass flow rate that maximizes efficiency is selected.

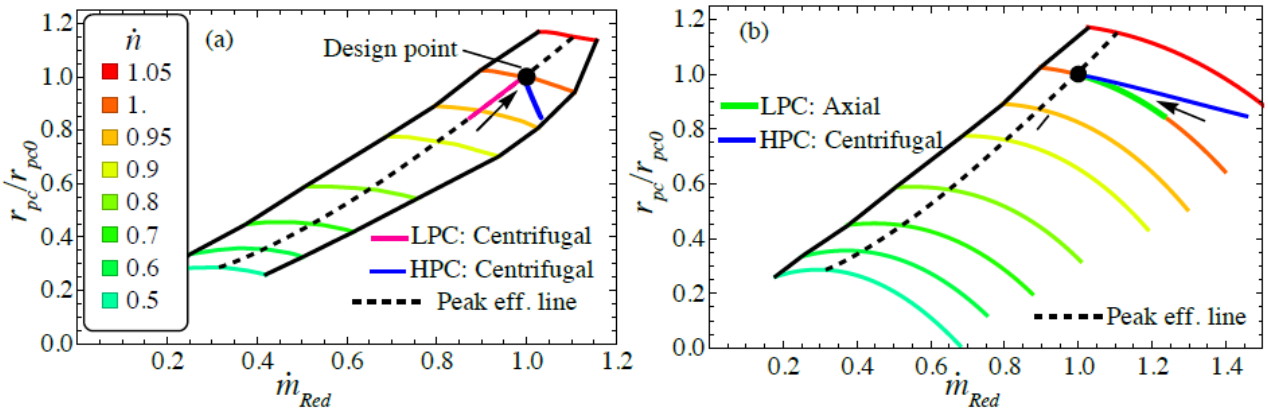

Figure 2. The compressors and turbines operate off-design. Using operating maps, the mass flow rates and efficiencies are determined as functions of the time-varying pressure within the cavern. (a) Operational maps considered for the case of two centrifugal compressors in series (see text), and (b) for the case of a hybrid axial-centrifugal compression train [7].

Figure 2 illustrates the two possible configurations for the compression train: (a) two centrifugal compressors, and (b) an axial LPC with a centrifugal HPC. The maximum efficiency line guides the simulation of the centrifugal compressor's behavior, ensuring that the operating point follows this trajectory as the cavern pressure increases, reaching the design point at the end of the charging process for at least one of the compressors (the LPC). This study employs operating maps obtained by interpolating data reported in [7]. The outlet pressure of the final compression stage is maintained slightly above the cavern pressure to prevent backflow or reverse air movement.

3. Thermo-economic optimization

A thermo-economic multi-objective optimization of an ACAES system is performed to determine the optimal decision variables of the analyzed plant configuration. The objective is to minimize both the capital expenditure and the levelized cost of storage. The optimization process is carried out using the genetic evolutionary algorithm NSGA-II.

3.1. Decision variables and bounds

In multi-objective optimization, the variables correspond to the set of initial parameters that can be modified to achieve optimal plant performance. The objective functions are those functions dependent on these variables that are sought to be optimized. In the context of ACAES system optimization, the decision variables are the system parameters that can be adjusted to meet the defined optimization objectives. In this work, the main decision variables selected include: the nominal air mass flow rates during charging and discharging ($\dot{m}_{c,0}$ y $\dot{m}_{d,0}$); the inner and outer radii (r_{in} y r_{out}) of the radial packed-bed (or thermal energy storage, TES); the layer ratio (LR) determining the internal composition of the storage material in the packed-bed; the aspect ratio (AR) of the packed-beds; the initial, maximum, and minimum cavern pressures ($p_{initial}$, p_{max} y p_{min}); and the pressure ratios across compressors and turbines (δp_c y δp_t). For further details, see Ref. [4]. The optimization is performed using a multi-objective NSGA-II algorithm. The constraints imposed on the system include: a minimum recoverable energy of 450 MWh during discharge, a maximum temperature variation at the turbine inlet of 120 °C, a nominal plant power of 150 MW, and charging and discharging times of approximately 3–4 hours per stage. For reference, the Huntorf plant is designed with a nominal power of 290 MW.

Table 1. *Main decision variables for the multi-objective optimization of the ACAES plant and their upper and lower bounds used in the optimization. See [8] for complete definitions and details.*

Variable	Symbol	Min.	Max.	Units
Nominal mass flow ratio (charge)	$\dot{m}_{c,0}$	350	600	(kg/s)
Nominal mass flow ratio (discharge)	$\dot{m}_{d,0}$	350	600	(kg/s)
TES length	$r_{out} - r_{in}$	7	35	(m)
TES internal radius	r_{in}	0	10	(m)
Layer ratio	LR	0	1	(-)
TES aspect ratio	AR	0.25	5	(-)
Initial pressure in cavern	$p_{initial}$	30	90	(atm)
Maximum pressure in cavern	p_{max}	40	75	(atm)
Minimum pressure in cavern	p_{min}	55	90	(atm)
Pressure ratio between compressors	δp_c	0.5	2.0	(-)
Pressure ratio between turbines	δp_t	0.5	2.0	(-)

3.2. Key performance indicators

The objective functions considered in this optimization, commonly referred to as key performance indicators (KPIs), are the capital investment (CAPEX) and the levelized cost of storage (LCoS), which are evaluated simultaneously. In a multi-objective optimization, KPIs can be formulated as quantities to be maximized or minimized; in this study, both are treated as functions to be minimized. CAPEX represents the total initial investment required for the construction of the plant. In turn, the Levelized Cost of Storage (LCoS) expresses the minimum average price at which the electricity generated must be sold to recover all costs over the assumed 30-year lifetime of the facility. The calculation of LCoS is based on four main factors: CAPEX, the capital recovery factor (CRF), operating expenses (OPEX), and the annual energy yield (AEY). The AEY, defined below, depends directly on the round-trip efficiency (RTE), defined as $RTE = E_{out}/E_{in}$ [9,10]. The LCoS is defined in Eq. (7):

$$LCoS = \frac{CAPEX \cdot CRF + OPEX}{AEY}. \quad (7)$$

The capital investment can be expressed as the sum of its components along with additional contingency and engineering factors:

$$CAPEX = C_{\text{land}} + (C_{\text{site}} + C_{\text{equipment}} + C_{\text{BOP}}) \cdot (1 + f_{\text{CONT}})(1 + f_{\text{EPC}}), \quad (8)$$

where C_{land} corresponds to the acquisition cost of the land designated for the plant. C_{site} represents the civil works costs required to prepare the site. $C_{equipment}$ encompasses the cost of the main plant equipment. C_{BOP} refers to the balance of plant cost, i.e., those systems and components necessary for operation but not directly linked to the main technology (such as electrical infrastructure, control systems, and auxiliaries). f_{CONT} is a contingency factor that accounts for uncertainties, risks, and unforeseen costs, assumed to be 7% in this work. f_{EPC} represents the costs associated with engineering, procurement, and construction, including design studies, system integration, quality assurance, labor management, logistics, profit margins, and risk premiums, assumed to be 13%. Inflation is estimated using the Marshall & Swift index [11]. The balance of plant costs is calculated as $C_{\text{BOP}} = c_{BOP} \cdot P_{gross}$, with $P_{gross} = 1.05 \cdot P_{out,net}$ and c_{BOP}=43$/kW. For the ACAES plant analyzed, the equipment costs can be disaggregated as follows (see Fig. 1):

$$C_{equipment} = C_{LPC} + C_{HPC} + C_{LPT} + C_{HPT} + C_{cavern} + C_{generator} + C_{HP-PB} + C_{LP-PB} + C_{HE} + C_{piping}. \quad (9)$$

The correlations used and the data sources for each of these terms are detailed in Table 2 [8]. The cost of the throttle valve is not considered in the analysis. For the LCoS calculation, it remains to determine the capital recovery factor (CRF), OPEX, and annual energy yield (AEY). The capital recovery factor is calculated as:

$$CRF = \frac{r\,(1+r)^N}{(1+r)^N+1}, \quad (10)$$

where r is the real discount rate, calculated from the nominal rate d and the interest rate i as: : $r = (1+d)/(1+i) - 1$ with d = 7% and i = 2.5% [9]. The plant lifetime, N, is assumed to be 30 years. The operating expenses (OPEX) include all costs associated with the operation and maintenance of the plant. Specifically, they consist of three components [12]: a fixed term proportional to the nominal output power, a variable term proportional to the annual energy yield (AEY), and a term associated with the cost of electricity purchased during the charging periods:

$$OPEX = C_{\text{OM,fix}} \cdot P_{\text{out,net}} + C_{\text{OM,prod}} \cdot AEY + C_{\text{el}} \cdot E_{\text{charging}}. \quad (11)$$

Table 2. *Main correlations used for calculating the costs associated with each component and turbomachinery. Here, $C_{rate,\$}$ is the USD-to-€ conversion factor, taken as $C_{rate,\$} = 0.86$.*

Component	Correlation	Refs.
Land and site	$C_{land} = c_{land} A_{land}$; $C_{site} = c_{site} A_{site}$	[9]
Pipes	$C_{piping} = f_{piping}\ C_{all,components}$	[9]
Axial compressor	$C_{LPC} = c_{comp}\, \dot{m}_{flow,ref} \left(\frac{\dot{m}_{flow}}{\dot{m}_{flow,ref}}\right)^{c,exp} r_{p,ref} log(r_p)\, f_c$	[9, 10]
Centrifugal compressor	$C_{LPC/HPC} = e^{\left\{9.1553 + 0.63\, log\left(\frac{P_c}{0.7457}\right)\right\}}\, C_{rate,\$}$	[11]
Axial turbine	$C_{LPC/HPC} = c_{turb} \dot{m}_{flow,ref} \left(\frac{\dot{m}_{flow}}{\dot{m}_{flow,ref}}\right)^{t,exp} r_{p,ref} log(r_p) f_t f_{T,turb}$	[9, 10]
Electric generator	$C_{generator} = C_{gen,ref}\, W_{gen}^{0.5463}$	[9]
HP- and LP-PBs	$C_{TES} = c_{material} V_{TES} + C_{tank} + \left(c_{HT,ins} V_{HT,ins} + c_{LT,ins} V_{LT,ins} + c_{tank} V_{tank}\right)$	[9]
PB tanks (pressure vessels)	$C_{tank} = (F_M\ C_v\ + C_{PL}) C_{rate,\$}$	[11]
Heat exchanger	$C_{HE} = 2835\ (\ 10.764\ A_{HE}\ )^{\{0.4\}}\ C_{rate,\$}$	[11]

Grid access fees are not included in the OPEX calculation due to their high variability, which depends on national regulations, connection configuration, installed capacity, and other site-specific conditions. The annual energy yield (AEY) and the total energy purchased during a year ($E_{charging}$) are calculated as:

$$AEY = \frac{365 \cdot 24}{t_{charge} + t_{discharge} + t_{idle}} E_{out,1cycle}, \quad (12)$$

$$E_{charging} = \frac{365 \cdot 24}{t_{charge} + t_{discharge} + t_{idle}} E_{in,1cycle}, \quad (13)$$

where $E_{out,1cycle}$ and $E_{in,1cycle}$ represent, respectively, the energy generated during each discharge cycle and the energy consumed during each charge cycle. One of the most complex cost components to estimate in an ACAES plant is the high-pressure air storage cavern. The term C_{cavern} includes costs associated with the geological site, its preparation, and measures required to ensure tightness. Initial stages may involve geophysical exploration, well drilling, leaching in salt caverns, cushion gas injection, lining and sealing, as well as surface control infrastructure. Although lined rock caverns have higher costs than salt caverns, thermal energy storage systems do not require extensive mechanical insulation, since they can be placed inside the cavern, avoiding high-pressure gradients. As a reference, the construction cost of a lined rock cavern of $3 \cdot 10^5\ \mathrm{m}^3$ is approximately €106 million, whereas a salt cavern of the same volume has a cost of around €32.5 million [8, 13].

In this study, different materials are analyzed for thermal energy storage (TES), including sensible heat storage materials and phase-change materials (PCM). Table 3 provides a list of the physical properties and specific costs of the materials considered, used for estimating $C_{\text{HP-PB}}$ and $C_{\text{LP-PB}}$.

Table 3. *Physical properties and cost of the materials used for thermal energy storage in the packed-beds.*

Material	Density [kg/m³]	Heat capacity [J/(kg·K)]	Conductivity [W/(m·K)]	$d_{p,in}$ / $d_{p,out}$ [cm]	$c_{material}$ [€/kg]
Commercial ceramic	2096	820	3.0	5/10	0.344
Alumina beads	3550	902	25	5/10	0.30
Copper slags	3600	1330	1.0	5/10	0.00
Steel slags	3500	950	1.5	5/10	0.00
Magnetite	5080	851	4.91	5/10	0.43
Quartzite	2500	830	3.16	5/10	0.03
Basalt	2640	1230	1.50	5/10	0.10
Adipic acid (PCM)	1360(s)-1093(l)	1590(s)-2260(l)	0.15	5/10	8.6
Solar salt (PCM)	1920	2300(s)-1420(l)	0.24	5/10	0.645
Pentaerythritol (PCM)	1161	2910(s)-2980(s)	0.387	5/10	2.32

4. Results

Various thermal energy storage materials have been analyzed for use in the packed-bed system. The corresponding Pareto fronts can be seen in Fig. 4. These materials include sensible heat storage materials such as basalt, magnetite, quartzite, aluminum oxide, and copper and steel slag. Additionally, the use of latent thermal energy storage materials based on solid–liquid phase change, such as adipic acid, was also investigated. Their different thermal properties and costs revealed a clear advantage of sensible storage materials over latent ones, particularly due to their lower cost-to-energy-density ratio. The results of the multi-objective optimization yield LCoS values below the threshold of 90 €/MWh, assuming an electricity purchase price of 50 €/MWh. For the CAPEX, values in the range of approximately 90–110 million € are obtained. Notably, copper and steel slags exhibit particularly favorable economic performance (see Fig. 4).

Figure 5 presents the plant optimization results for two compression train configurations: one consisting of two centrifugal compressors, and another combining one axial compressor with one centrifugal compressor. The fully centrifugal configuration demonstrates superior economic optimization across most of the CAPEX range. However, under certain conditions—such as scenarios involving very low initial investment—the axial–centrifugal configuration may become more advantageous.

5. Conclusions

In the original diabatic Huntorf plant, which uses a natural gas combustion chamber, the overall round-trip efficiency (RTE) reaches a value of 0.42. By incorporating a packed-bed thermal storage system—i.e., converting the plant into an adiabatic ACAES—with dimensions (energy and power) comparable to Huntorf, the modeled efficiency in this work increases to RTE = 0.79.

Regarding the packed-bed storage materials, copper and steel slags provide the best combination of thermodynamic efficiency and economic performance. Within the context of the European Union, steel slag is particularly abundant in mineral processing industries and can therefore be reused for energy storage purposes.

Concerning the ACAES plant's compression train during charging, a configuration consisting of two centrifugal compressors (C+C) achieves lower LCoS values across almost the entire Pareto front, outperforming the multi-objective optimization of a compression train that combines axial and centrifugal compressors (A+C).

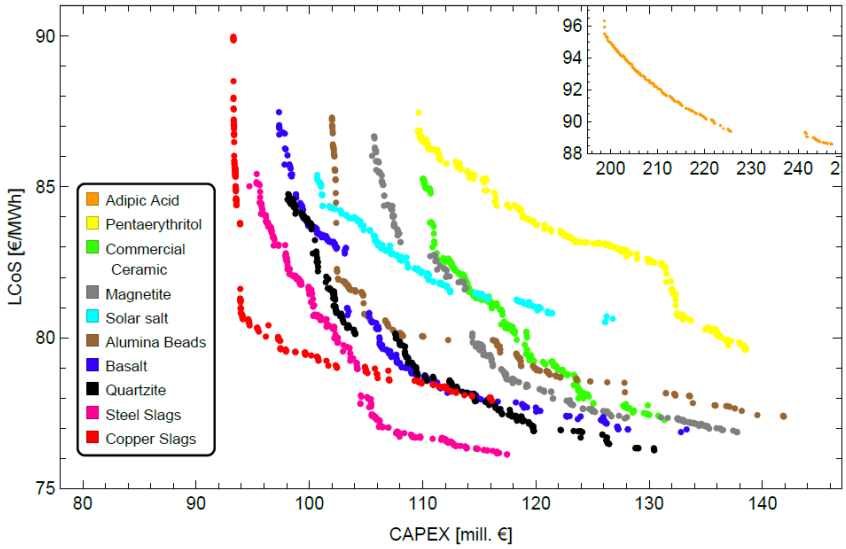

Figure 4. *Pareto fronts obtained from the multi-objective optimization of the ACAES plant shown in Fig. 1. Different packed-bed storage materials are represented.*

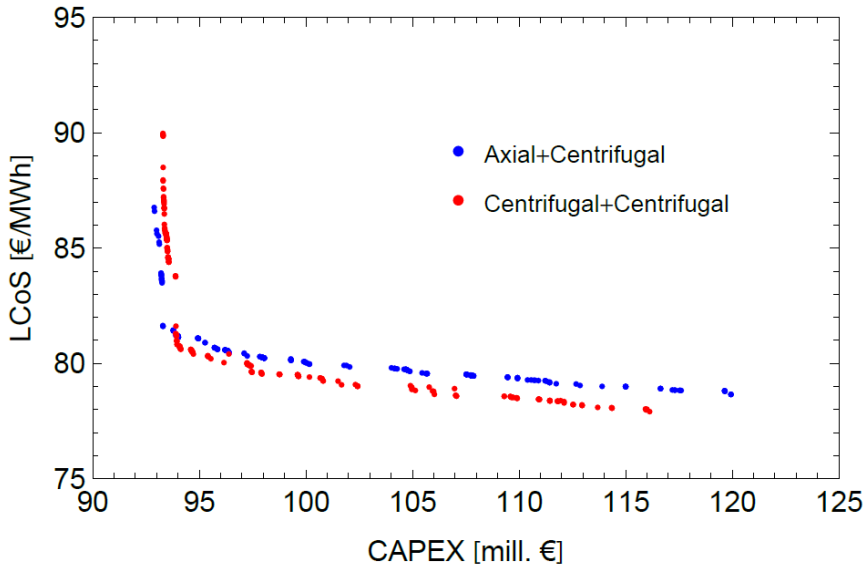

Figure 5. *Pareto fronts for the multi-objective optimization. The compression train considered is either axial + centrifugal or centrifugal + centrifugal. The storage material used is copper slag.*

References

[1] Barbour E., Pottie D. L. Adiabatic compressed air energy storage technology. Joule 2021; 5, 1914 – 1920

[2] Sciacovelli A., Li Y., Chen H., Wu Y., Wang J., Garvey S., Ding Y. (). Dynamic simulation of adiabatic compressed air energy storage (ACAES) plant with integrated thermal storage - Link between components performance and plant performance. Appl. Ener. 2017; 185, 16–28.

[3] Mersch, M., Sapin, P., Olympios, A. V., Ding, Y., Mac Dowell, N., Markides, C. N. A unified framework for the thermo-economic optimisation of compressed-air energy storage systems with solid and liquid thermal stores. Energy Conversion and Management. 2023; 287, 117061.

[4] Pérez-Gallego, D., Gonzalez-Ayala, J., Medina, A., Calderón-Vásquez, I., Hernández, A. C. Full dynamic simulation of an adiabatic compressed air energy storage plant with radial-flow packed-bed storage and an organic Rankine cycle unit. Energy Conversion and Management 2026; 348, 120764.

[5] Pérez-Gallego, D., Gonzalez-Ayala, J., Medina, A., Hernández, A. C. Comprehensive review of dynamical simulation models of packed-bed systems for thermal energy storage applications in renewable power production. Heliyon 2025; 11(4) e42803.

[6] Dixon, S. L., Hall, C. Fluid mechanics and thermodynamics of turbomachinery. Butterworth-Heinemann; 2013.

[7] Giostri, A., Macchi, E. An advanced solution to boost sun-to-electricity efficiency of parabolic dish. Solar Energy 2016; 139, 337-354.

[8] Pérez-Gallego, D., González Ayala, J., Medina Domínguez, A., Anvari, S., Calderón-Vásquez, I., Cardemil, J. M., Calvo Hernández, A. Thermo-economic optimization of an adiabatic compressed air energy storage system including system dynamics. Journal of Energy Storage 2026; 153, 121114.

[9] Guccione, S., Guedez, R. Techno-economic optimization of molten salt based CSP plants through integration of supercritical CO2 cycles and hybridization with PV and electric heaters. Energy 2023; 283, 128528.

[10] Spelling, J. Hybrid solar gas-turbine power plants: a thermoeconomic analysis. Doctoral dissertation, KTH Royal Institute of Technology, 2013.

[11] Seider, W. D., Lewin, D. R., Seader, J. D., Widagdo, S., Gani, R., Ng, K. M. Product and process design principles: synthesis, analysis and evaluation. John Wiley & Sons 2016.

[12] Black & Veatch Engineering. Cost and performance data for power generation technologies, National Renewable Energy Laboratory (NREL); 2012. Report.

[13] Papadias, D. D., Ahluwalia, R. K. Bulk storage of hydrogen. International Journal of Hydrogen Energy 2021; 46(70), 34527-34541.